

Abstract

This thesis investigates the role that synchronization plays in protecting neurons from noise and degradation in a control-theoretic model of the human cerebellum. Some of the foundational concepts and theorems in synchronization theory are covered. The main results of this paper include modeling a network of diffusively coupled linear neurons which could implement part of the cerebellum model and deriving synchronization conditions for that model. In addition, modified synchronization conditions are presented for a more detailed model, and simulations are conducted to verify some results and shed light on a more general context which is less amenable to direct analysis.

Keywords— Synchronization, Control Theory, Linear Systems, Neuroscience

Acknowledgments

First and foremost, I would like to thank my supervisor Professor Mireille Broucke for her support and mentorship. Working with her has had a profound impact on me and shaped my nascent research interests. Wherever I go from here, I will owe it to her.

I am also grateful to the Professors, TA's, and peers who all went above and beyond to support me throughout my undergraduate career. I hope to one day pay forward the generosity, patience, and kindness they have all offered me.

In addition, I am forever grateful to my friends, and everyone who has contributed to the vibrant community here at UofT. From the organizers of events like Frosh Week to my roommates Jon and Navin, and anyone who has offered a shoulder to lean on, a voice on the line, a soft catch when I fall, or hustled on the back-check: thank you.

To my best friend Raysa, I couldn't ask for a better partner. I can't wait to see where life takes us. Finally, to my family, each of whom has been at times teacher, role-model, cheerleader, companion, and so much more. I would certainly not be here without you.

Contents

1	Introduction	1
2	Background	1
2.1	Motivation	1
2.2	Wu and Chua’s Framework	3
2.2.1	Setup	3
2.2.2	Lyapunov’s Direct Method	4
2.2.3	Selection of \mathbf{M}	6
2.2.4	Diagonal \mathbf{D}_{ij}	7
2.2.5	Normal $\tilde{\mathbf{D}}_{ii}$	8
2.3	The Kuramoto Model	10
2.4	Contraction Analysis	11
2.5	Noisy Coupled Systems	14
2.6	Diffusion	15
3	Results	16
3.1	Modeling Neuron Interactions	16
3.2	Synchronization in Neuron Model	18
3.3	Main result for linear systems	18
3.4	Simulations	20
3.4.1	Methods	20
3.4.2	Simulation Results and Discussion	20
4	Further Work	23
5	Conclusion	24
A	Additional Results from Wu and Chua	27
A.1	Reducible Coupling Matrix	27
A.2	Nonlinear Additive Coupling	29
B	Simulation Code	30

List of Figures

1	Parallel computation of filtering	3
2	Example k-connected ring	17
3	Simulation results for error vs k	21
4	Simulation results for error vs noise	22
5	Simulation results for error vs m	23
6	Strongly connected graph example	27

Notation and Terminology

Throughout this paper, we adopt the following notation:

- Scalar values will be denoted by lowercase, ex: t
- Vectors will be denoted by bold lowercase, ex: \mathbf{x}
- Matrices will be denoted by bold uppercase, ex: \mathbf{M}
- $\|*\|$ denotes the Euclidean norm of $*$
- We denote the set $\{\alpha\mathbf{I}_k : \alpha \in \mathbb{R}\}$ as \mathcal{F}_k , where \mathbf{I}_k is the $k \times k$ identity matrix
- $\mathbf{0}$ will refer to either the 0 vector or 0 matrix, which should be inferred from context
- We denote the set of $n \times m$ matrices with entries in set \mathcal{S} as $\mathcal{M}_{n \times m}(\mathcal{S})$.
 - Sometimes, instead of writing $\mathbf{A} \in \mathbb{R}^{n \times m}$ we instead write $\mathbf{A} \in \mathcal{M}_{n \times m}(\mathbb{R}^{k \times k})$ to suggest that \mathbf{A} be interpreted as an $n \times m$ matrix (of $k \times k$ real-valued blocks)
- (Block) diagonal matrices will sometimes be written as $\text{diag}(\mathbf{A}, \mathbf{B}, \dots)$
- A group of coupled systems is equivalently called an “array”, “network”, or “supersystem”
- An individual system in an array is equivalently called a “cell” or “subsystem”.

1 Introduction

While modern robots excel in a range of applications such as manufacturing and agriculture, they still struggle to match human-like fluidity and adaptability when it comes to certain tasks [1]. Fortunately, engineers have access to a blueprint for a control design with a demonstrated capacity to learn and adaptively interact with its environment: the human brain. Thus, it is valuable to develop models of the brain which might provide insights into how we can invent new control designs. Such models ideally would be biologically feasible, meaning that it should be possible to explain how they are implemented by biological components. The goal of this paper is to examine one such model, and attempt to prove one aspect of its biological feasibility, namely the issue of synchronization. In particular, we will discuss why synchronization is important to the feasibility of this design, and then study synchronization from a control perspective. Finally, we will attempt to derive a set of conditions which would enable us to prove that synchronization will occur.

2 Background

2.1 Motivation

In 2022, Broucke published a monograph titled “Adaptive Internal Models in Neuroscience” which proposed a theoretical model for the function of the human cerebellum in disturbance rejection [2]. In particular, when applied to the slow eye movement subsystem of the cerebellum, her model could replicate a wide range of human oculomotor behavior. The model is shown below:

$$\dot{\hat{x}} = -K_x \hat{x} + u \quad (1a)$$

$$\dot{w}_0 = Fw_0 + FGe \quad (1b)$$

$$\dot{w}_1 = Fw_1 - Ge \quad (1c)$$

$$\dot{w}_2 = Fw_2 - Gu_s \quad (1d)$$

$$\dot{w}_3 = Fw_3 - Gu_{im} \quad (1e)$$

$$\hat{w}_d := (w_0 + Ge, w_1, w_2, w_3) \quad (1f)$$

$$\dot{\hat{\psi}}_d = e\hat{w}_d^T \quad (1g)$$

$$u_b = \alpha_x \hat{x} - \alpha_{VOR} \dot{x}_h \quad (1h)$$

$$u_s = K_e e \quad (1i)$$

$$u_{im} = \hat{\psi}_d \hat{w}_d \quad (1j)$$

$$u = u_b + u_s + u_{im} \quad (1k)$$

A subtle issue arises when considering how such a design is implemented in neural circuitry. The design requires that in equations (1b) - (1e), the controllable pair (F, G) is identical across each filter. What mechanism guarantees that each filter has the same copy of F and G ? With digital or electronic designs, it would be trivial to set these matrices explicitly, but on neural hardware it's not so simple. Such a mechanism would need to be robust to noise, as well as to degradation due to fatigue, stress, etc. We pose the following question:

Question 1. In Broucke's model for the slow eye movement system, what mechanism maintains the pair (F, G) across the filters (1b) - (1e)?

Additionally neuroscience literature suggests that each filter is not computed at a single point, a single time, but rather is carried out in parallel by many redundant groups of cells, and then averaged [3], as shown in Figure 1. This design is hypothesized to confer robustness and enhanced precision to the computation of each filter. However, Tabareau and Slotine show in [4] that in order for averaging across noisy systems to produce a meaningful result, the systems must be *synchronized* (a property which is defined in greater detail later in this paper). This hints at a possible solution to Question 1, and raises another interesting question:

Question 2. What conditions must be satisfied for the parallel filters in Broucke's model to asymptotically synchronize? Furthermore, precisely how much is the impact of noise and

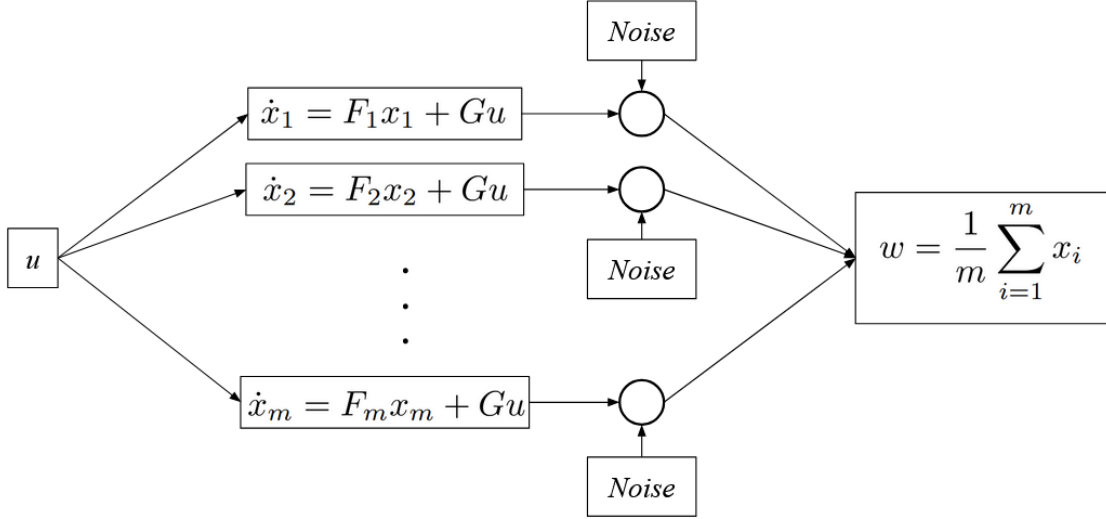


Figure 1: Parallel computation of filtering

perturbation reduced by synchronization?

Originally, this thesis aimed to answer both questions, but ultimately settled on exploring and understanding the answer to question 2.

2.2 Wu and Chua’s Framework

In 1995, Wu and Chua published a series of papers on synchronization, including “Synchronization in an array of linearly coupled dynamical systems” [5] and “A Unified Framework for Synchronization and Control of Dynamical Systems” [6]. These papers contributed foundational results in the study of synchronization, which this section will summarize for our purposes. Much of the notation, terminology, and setup introduced here are reused in later sections.

2.2.1 Setup

To begin, consider m identical nonlinear systems (individual “cells”) each of order n , diffusively coupled with each other (constituting an “array”).

$$\dot{\mathbf{x}}_i = \mathbf{f}(\mathbf{x}_i, t) + \sum_{j=1}^m \mathbf{K}_{ij}(\mathbf{x}_j - \mathbf{x}_i) \quad i = 1 \dots m \quad (2)$$

Let $-\mathbf{D}$ represent the Laplacian matrix [7] of this network. That is, $\mathbf{D}_{ii} = -\sum_j \mathbf{K}_{ij}$, and $\mathbf{D}_{ij} = \mathbf{K}_{ij}$ for $i \neq j$. Further, define $\bar{\mathbf{x}} = [\mathbf{x}_1^T \quad \mathbf{x}_2^T \quad \dots \quad \mathbf{x}_m^T]^T$ and let $\bar{\mathbf{f}}(\bar{\mathbf{x}}, t) =$

$$\left[\mathbf{f}(\mathbf{x}_1, t)^T \quad \mathbf{f}(\mathbf{x}_2, t)^T \quad \dots \quad \mathbf{f}(\mathbf{x}_m, t)^T \right]^T$$

we can rewrite array (2) as the compact system

$$\dot{\mathbf{x}} = \bar{\mathbf{f}}(\mathbf{x}) + \mathbf{D}\mathbf{x} \quad \in \mathbb{R}^{nm} \quad (3)$$

An important property of the Laplacian matrix \mathbf{D} is that the sum along any row is $\mathbf{0}$, i.e. $\sum_{j=1}^m \mathbf{D}_{i,j} = \mathbf{0}$, $i = 1 \dots m$. This means that when $\mathbf{x}_1 = \mathbf{x}_2 = \dots = \mathbf{x}_m$, the coupling term $\mathbf{D}\bar{\mathbf{x}} = \mathbf{0}$. Thus, when the array is synchronized, the coupling forces are 0 and each cell is effectively uncoupled. Now, consider the following definitions which provide a “first principles” approach to synchronization.

Definition 2.1 (Uniform Synchronization [5]). System (2) is uniformly synchronized if for each $\epsilon > 0$, there exists $\delta(\epsilon) > 0$ such that if $\|\mathbf{x}_i(0) - \mathbf{x}_j(0)\| \leq \delta(\epsilon)$, then $\|\mathbf{x}_i(t) - \mathbf{x}_j(t)\| \leq \epsilon$ for all t , and all $i, j = 1 \dots m$.

Definition 2.2 (Uniform Asymptotic Synchronization [5]). System (2) is uniformly asymptotically synchronized if it is uniformly synchronized and $\lim_{t \rightarrow \infty} \|\mathbf{x}_i(t) - \mathbf{x}_j(t)\| = 0$ for all $i, j = 1 \dots m$.

2.2.2 Lyapunov’s Direct Method

Wu and Chua approach the problem of synchronization using Lyapunov’s direct method [8], a tool for analyzing stability of nonlinear systems. The way it is applied here is to define a function $\mathbf{d}(\bar{\mathbf{x}})$ which measures the “distance” between cells. Then, we will use Lyapunov’s method to determine conditions on the stability of $\mathbf{d}(\bar{\mathbf{x}})$, thereby determining conditions for synchronization of array (2).

One potential choice of $\mathbf{d}(\bar{\mathbf{x}})$ is

$$\mathbf{d}(\bar{\mathbf{x}}) = \begin{bmatrix} \mathbf{I} & -\mathbf{I} & & & & \\ & \mathbf{I} & -\mathbf{I} & & & \\ & & \ddots & \ddots & & \\ & & & \mathbf{I} & -\mathbf{I} & \\ & & & & & \end{bmatrix} \bar{\mathbf{x}} = \mathbf{M}\bar{\mathbf{x}} \quad (4)$$

A theorem in [5] states that the array (2) is uniformly asymptotically synchronized if $\mathbf{d}(\bar{\mathbf{x}})$ is uniformly asymptotically stable. They additionally derive conditions for the stability of

$\mathbf{d}(\bar{\mathbf{x}})$, which are provided in the following theorem.

Theorem 1. Suppose there exists $n \times n$ matrices \mathbf{T} and \mathbf{Q} with \mathbf{Q} symmetric positive definite [9] and $c > 0$ such that for all $t > 0$, $\mathbf{a}, \mathbf{b} \in \mathbb{R}^n$, the following inequality holds

$$(\mathbf{a} - \mathbf{b})\mathbf{Q}\left(\mathbf{f}(\mathbf{a}, t) - \mathbf{T}\mathbf{a} - (\mathbf{f}(\mathbf{b}, t) - \mathbf{T}\mathbf{b})\right) \leq -c\|\mathbf{a} - \mathbf{b}\| \quad (5)$$

Further suppose that the following matrix is negative semidefinite [9]

$$\mathbf{M}^T \begin{bmatrix} \mathbf{Q} & & & \\ & \mathbf{Q} & & \\ & & \ddots & \\ & & & \mathbf{Q} \end{bmatrix} \mathbf{M} \left(\mathbf{D} + \begin{bmatrix} \mathbf{T} & & & \\ & \mathbf{T} & & \\ & & \ddots & \\ & & & \mathbf{T} \end{bmatrix} \right) \quad (6)$$

Then the array (2) is uniformly asymptotically synchronized.

Proof. Consider the following Lyapunov function candidate [8] for $\mathbf{d}(\bar{\mathbf{x}})$

$$V(\mathbf{d}(\bar{\mathbf{x}})) = \bar{\mathbf{x}}^T \mathbf{M}^T \begin{bmatrix} \mathbf{Q} & & & \\ & \mathbf{Q} & & \\ & & \ddots & \\ & & & \mathbf{Q} \end{bmatrix} \mathbf{M} \bar{\mathbf{x}} = \bar{\mathbf{x}}^T \mathbf{U} \bar{\mathbf{x}} \quad (7)$$

The derivative along solutions of (7) is $\dot{V}(\mathbf{d}(\bar{\mathbf{x}})) = \bar{\mathbf{x}}^T \mathbf{U} (\bar{\mathbf{f}}(\bar{\mathbf{x}}) + \mathbf{D}\bar{\mathbf{x}})$. Adding $(\text{diag}(\mathbf{T}, \mathbf{T}, \dots, \mathbf{T}) - \text{diag}(\mathbf{T}, \mathbf{T}, \dots, \mathbf{T}))\bar{\mathbf{x}} = \mathbf{0}$ simplifies to

$$\dot{V}(\mathbf{d}(\bar{\mathbf{x}})) = \bar{\mathbf{x}}^T \mathbf{U} \begin{bmatrix} \mathbf{f}(\mathbf{x}_1) - \mathbf{T}\mathbf{x}_1 \\ \vdots \\ \mathbf{f}(\mathbf{x}_m) - \mathbf{T}\mathbf{x}_m \end{bmatrix} + \bar{\mathbf{x}}^T \mathbf{U} \left(\mathbf{D} + \begin{bmatrix} \mathbf{T} & & & \\ & \mathbf{T} & & \\ & & \ddots & \\ & & & \mathbf{T} \end{bmatrix} \right) \bar{\mathbf{x}}$$

By condition (5), the left term is negative definite, and by condition (6), the right term is negative semi-definite. Thus, the derivative along solutions of equation (7) is negative definite and by Lyapunov's direct method, $\mathbf{d}(\bar{\mathbf{x}})$ is asymptotically stable [8]. Further, we can use the fact that if $\mathbf{d}(\bar{\mathbf{x}})$ is asymptotically stable then array (2) is asymptotically synchronized to

conclude the proof. □

Note that there is considerable flexibility with how the matrices can be chosen. Namely, if we can find *any* \mathbf{T} , \mathbf{Q} satisfying the conditions (5) and (6), then we have shown that system (2) is uniformly asymptotically synchronized. We will also see that there are alternative ways of writing \mathbf{M} which allow us to simplify the analysis.

2.2.3 Selection of \mathbf{M}

Recall that the key requirement for the definition of $\mathbf{d}(\bar{\mathbf{x}})$ in equation (4) was that $\mathbf{d}(\bar{\mathbf{x}}) \rightarrow 0$ if and only if $\|\mathbf{x}_i - \mathbf{x}_j\| \rightarrow 0$ for all i, j from $1 \dots m$. Preserving the form $\mathbf{d}(\bar{\mathbf{x}}) = \mathbf{M}\bar{\mathbf{x}}$, it turns out that there are many suitable choices for \mathbf{M} which satisfy this requirement. For example, we could select

$$\mathbf{M} = \begin{bmatrix} \mathbf{I} & -\mathbf{I} & & & \\ & \mathbf{I} & -\mathbf{I} & & \\ & \vdots & & \ddots & \\ & \mathbf{I} & & & -\mathbf{I} \end{bmatrix} \in \mathcal{M}_{m-1 \times m}(\mathcal{F}_n)$$

Which corresponds to the sum $d(\mathbf{x}) = \sum_{i=2}^m \|\mathbf{x}_1 - \mathbf{x}_i\|^2$. This motivates us to define the following classes of matrices which can be used in equation (4):

Definition 2.3 ($M_1(k)$). Matrices in the class $M_1(k)$ are matrices \mathbf{M} with entries in \mathcal{F}_k such that each row contains zeros and exactly one $\alpha\mathbf{I}_k$ and one $-\alpha\mathbf{I}_k$ for a nonzero real α . We may interpret the matrix $\mathbf{M} \in M_1(k)$ to represent an undirected graph: for each column of \mathbf{M} define a vertex, and for each row define an edge between vertex i and vertex j where i and j are the indices for the two non-zero elements in that row.

Definition 2.4 ($M_2(k)$). Matrices in the class $M_2(k)$ are matrices in $M_1(k)$ for which the graph they represent is connected. That is, for any k, j in $1 \dots m$, the graph contains a path from k to j . Note that if \mathbf{M} is a $p \times m$ matrix in $M_2(k)$, then $p \geq m - 1$

With the above definitions, it turns out that any matrix $\mathbf{M} \in M_2(n)$ can be used in the definition of $d(\mathbf{x})$ in (4).

Theorem 2. If conditions (5) and (6) hold for any $\mathbf{M} \in M_2(n)$, then the array (2) is uniformly asymptotically synchronized.

The fact that both \mathbf{M} and the coupling matrix \mathbf{D} can be interpreted as representing a graph

is suggestive of how we might select \mathbf{M} in some cases, as we will see in section 2.2.5.

2.2.4 Diagonal \mathbf{D}_{ij}

Diagonal \mathbf{D}_{ij} corresponds to an array where the coupling term for the k th state of each cell is a linear function of the k th state of each other cell. This motivates us to permute $\bar{\mathbf{x}}$ in such a way that the k th state of each cell is collected into a vector $\tilde{\mathbf{x}}_k \in \mathbb{R}^m$, and $\tilde{\mathbf{x}} = \begin{bmatrix} \tilde{\mathbf{x}}_1^T & \tilde{\mathbf{x}}_2^T & \dots & \tilde{\mathbf{x}}_n^T \end{bmatrix}^T$. This allows us to rewrite the dynamics of array (2) as

$$\dot{\tilde{\mathbf{x}}}_i = \tilde{\mathbf{f}}_i(\tilde{\mathbf{x}}) + \tilde{\mathbf{D}}_{ii}\tilde{\mathbf{x}}_i \quad i = 1 \dots n \quad (8)$$

The property of the original system that the sum along any row of \mathbf{D} is $\mathbf{0}$ is reflected in the fact that the sum along any row of $\tilde{\mathbf{D}}_{ii}$ is 0.

For systems with uniformly bounded Jacobians, we can additionally impose the restriction that \mathbf{Q} and \mathbf{T} are diagonal. Specifically, $\mathbf{Q} = \text{diag}(q_1, q_2, \dots, q_n)$ and $\mathbf{T} = \text{diag}(t_1, t_2, \dots, t_n)$. Additionally, define $\tilde{\mathbf{M}} \in M_2(1)$ as the real valued matrix obtained by replacing \mathbf{I} with 1 in \mathbf{M} .

Theorem 3. Suppose \mathbf{D}_{ij} is diagonal for each $i, j = 1 \dots m$. Consider the permuted system (8). If there exists a positive definite diagonal matrix \mathbf{Q} and diagonal matrix \mathbf{T} , such that condition (5) holds, and additionally there exists a matrix $\tilde{\mathbf{M}} \in M_2(1)$ such that $\tilde{\mathbf{M}}^T \tilde{\mathbf{M}} (\tilde{\mathbf{D}}_{ii} + t_i \mathbf{I}_m)$ is negative semi-definite for all i , then system (2) is uniformly asymptotically synchronized.

Proof.

$$\begin{aligned}
& \mathbf{x}^T \mathbf{U} \left(\mathbf{D} + \begin{bmatrix} \mathbf{T} & & & \\ & \mathbf{T} & & \\ & & \ddots & \\ & & & \mathbf{T} \end{bmatrix} \right) \mathbf{x} \\
&= \tilde{\mathbf{x}}^T \begin{bmatrix} q_1 \tilde{\mathbf{M}}^T \tilde{\mathbf{M}} (\tilde{\mathbf{D}}_{11} + t_1 \mathbf{I}_m) & & & \\ & q_2 \tilde{\mathbf{M}}^T \tilde{\mathbf{M}} (\tilde{\mathbf{D}}_{22} + t_2 \mathbf{I}_m) & & \\ & & \ddots & \\ & & & q_n \tilde{\mathbf{M}}^T \tilde{\mathbf{M}} (\tilde{\mathbf{D}}_{nn} + t_n \mathbf{I}_m) \end{bmatrix} \tilde{\mathbf{x}} \\
&= \sum_{i=1}^n q_i \tilde{\mathbf{x}}_i^T \tilde{\mathbf{M}}^T \tilde{\mathbf{M}} (\tilde{\mathbf{D}}_{ii} + t_i \mathbf{I}_m) \tilde{\mathbf{x}}_i \tag{9}
\end{aligned}$$

Thus, it is sufficient to verify that $\tilde{\mathbf{M}}^T \tilde{\mathbf{M}} (\tilde{\mathbf{D}}_{ii} + t_i \mathbf{I}_m)$ is negative semi-definite for all i to show asymptotic synchronization of system (2). \square

2.2.5 Normal $\tilde{\mathbf{D}}_{ii}$

These synchronization conditions can be further relaxed when we make stronger assumptions. Specifically, assumption **A1** is a condition on the form of the network, assumption **A2** states that the coupling between states is similar up to a scaling factor, assumption **A3** requires the network to be connected, assumptions **A4** and **A5** are automatically satisfied by diffusive networks, and assumption **A6** is a condition on the strength of the connections. While it may appear that these are excessively restrictive conditions, in practical applications they can often be easily verified, as we will see later in section 3.2.

Theorem 4. For system (2) with diagonal \mathbf{D}_{ij} , if for each i , either $\tilde{\mathbf{D}}_{ii} = \mathbf{0}$ and $t_i \leq 0$ or $\tilde{\mathbf{D}}_{ii}$ satisfies all of the following assumptions

A1 $\tilde{\mathbf{D}}_{ii}$ is normal ($\tilde{\mathbf{D}}_{ii}^T \tilde{\mathbf{D}}_{ii} = \tilde{\mathbf{D}}_{ii} \tilde{\mathbf{D}}_{ii}^T$)

A2 $\alpha_{ij} (\tilde{\mathbf{D}}_{ii} + \tilde{\mathbf{D}}_{ii}^T) = \tilde{\mathbf{D}}_{jj} + \tilde{\mathbf{D}}_{jj}^T$ for a real number α_{ij} for each j in $1 \dots n$

A3 $\tilde{\mathbf{D}}_{ii} + \tilde{\mathbf{D}}_{ii}^T$ is irreducible

A4 The sum along any row of $\tilde{\mathbf{D}}_{ii} + \tilde{\mathbf{D}}_{ii}^T$ is 0

A5 $\tilde{\mathbf{D}}_{ii} + \tilde{\mathbf{D}}_{ii}^T$ is a Metzler matrix

A6 Each eigenvalue of $\tilde{\mathbf{D}}_{ii}$ with nonzero real part has real part less than or equal to $-t_i$ then system (2) is asymptotically synchronized.

Proof. We start by assuming $\tilde{\mathbf{D}}_{i,i}$ is nonzero, and relax this condition at the end.

Note that for matrices $\mathbf{M} \in M_1(k)$, the symmetric matrix $-(\mathbf{M}^T \mathbf{M})$ is a Metzler matrix for which the sum of entries along each row is equal to $\mathbf{0}$. If $\mathbf{M} \in M_2(k)$, then $-(\mathbf{M}^T \mathbf{M})$ is irreducible. The converse holds for real valued matrices: a matrix $\mathbf{A} \in \mathbb{R}^{m \times m}$ is symmetric, Metzler, irreducible, and has row-sums equal to 0 if and only if there exists an $\mathbf{M} \in M_2(1)$ such that $\mathbf{A} = -(\mathbf{M}^T \mathbf{M})$.

Using assumption **A2**, this fact motivates us to select $\tilde{\mathbf{M}}$ satisfying $-\alpha_1(\tilde{\mathbf{D}}_{1,1} + \tilde{\mathbf{D}}_{1,1}^T) = \dots = -\alpha_n(\tilde{\mathbf{D}}_{n,n} + \tilde{\mathbf{D}}_{n,n}^T) = \tilde{\mathbf{M}}^T \tilde{\mathbf{M}}$, where $\alpha_1 \dots \alpha_n$ are real positive numbers. To test the negative semi-definiteness of (9), we construct

$$\begin{aligned} & \tilde{\mathbf{M}}^T \tilde{\mathbf{M}}(\tilde{\mathbf{D}}_{i,i} + t_i \mathbf{I}_m) + (\tilde{\mathbf{M}}^T \tilde{\mathbf{M}}(\tilde{\mathbf{D}}_{i,i} + t_i \mathbf{I}_m))^T \\ &= -\alpha_i(\tilde{\mathbf{D}}_{i,i} + \tilde{\mathbf{D}}_{i,i}^T)(\tilde{\mathbf{D}}_{i,i} + t_i \mathbf{I}_m) + (-\alpha_i(\tilde{\mathbf{D}}_{i,i} + \tilde{\mathbf{D}}_{i,i}^T)(\tilde{\mathbf{D}}_{i,i} + t_i \mathbf{I}_m))^T \\ &= -\alpha_i(\tilde{\mathbf{D}}_{i,i} + \tilde{\mathbf{D}}_{i,i}^T)(\tilde{\mathbf{D}}_{i,i} + \tilde{\mathbf{D}}_{i,i}^T + 2t_i \mathbf{I}_m) \end{aligned} \quad (10)$$

In order for (10) to be negative semi-definite, we must have $(\tilde{\mathbf{D}}_{i,i} + \tilde{\mathbf{D}}_{i,i}^T)(\tilde{\mathbf{D}}_{i,i} + \tilde{\mathbf{D}}_{i,i}^T + 2t_i \mathbf{I}_m)$ positive semi-definite. As this is a symmetric matrix, we can simply check that all it's eigenvalues are non negative. A theorem from the original paper [5] states that for matrices $\tilde{\mathbf{D}}_{i,i}$ satisfying the above properties, the eigenvalues of $\tilde{\mathbf{D}}_{i,i} + \tilde{\mathbf{D}}_{i,i}^T$ are always non-positive. By the spectral mapping theorem, the eigenvalues of $(\tilde{\mathbf{D}}_{i,i} + \tilde{\mathbf{D}}_{i,i}^T)(\tilde{\mathbf{D}}_{i,i} + \tilde{\mathbf{D}}_{i,i}^T + 2t_i \mathbf{I}_m)$ are non negative if the nonzero eigenvalues of $(\tilde{\mathbf{D}}_{i,i} + \tilde{\mathbf{D}}_{i,i}^T)$ are less than or equal to $-2t_i$. Since $\tilde{\mathbf{D}}_{i,i}$ is normal, the eigenvalues of $(\tilde{\mathbf{D}}_{i,i} + \tilde{\mathbf{D}}_{i,i}^T)$ are 2 times the real part of the eigenvalues of $\tilde{\mathbf{D}}_{i,i}$. So in order to show asymptotic synchronization, we can show that any eigenvalue of $\tilde{\mathbf{D}}_{i,i}$ with nonzero real part has real part less than or equal to $-t_i$ for all $i \in 1 \dots n$.

Finally, we can relax our assumption to allow $\tilde{\mathbf{D}}_{i,i} = \mathbf{0}$ by observing that in that case $\tilde{\mathbf{M}}^T \tilde{\mathbf{M}}(\tilde{\mathbf{D}}_{i,i} + t_i \mathbf{I}_m) = t_i \tilde{\mathbf{M}}^T \tilde{\mathbf{M}}$. Since we have seen that the eigenvalues of $\tilde{\mathbf{M}}^T \tilde{\mathbf{M}}$ are always non-negative, we conclude the proof. \square

These results require irreducible coupling matrices, which we may not always have. Appendix A looks at how we can partition the original system into irreducible sub-components which

can be analyzed independently, so that the results of this section can still be applied.

2.3 The Kuramoto Model

One powerful framework for analyzing synchronization phenomena is the Kuramoto model, developed in 1975. In 2000, Strogatz published a survey of key results and open problems (at the time) surrounding the model [10]. This section will summarize some of those basic results.

The Kuramoto model describes N limit cycle oscillators with all-to-all sinusoidal coupling with coupling strength K as follows:

$$\dot{\theta}_k = \omega_k + \sum_{j=1}^N \frac{K}{N} \sin(\theta_j - \theta_k), \quad k = 1 \dots N \quad (11)$$

Each ω_i is assumed to be drawn from a Gaussian distribution $g(\omega)$. We define the *order parameter* as follows:

$$r e^{i\psi} = \frac{1}{N} \sum_{j=1}^N e^{i\theta_j} \quad (12)$$

where r is the *coherence* and ψ is the average phase. Multiplying both sides by $e^{-i\theta_k}$ and equating complex parts yields the following mean-field characterization of the Kuramoto model:

$$\dot{\theta}_k = \omega_k + K r \sin(\psi - \theta_k), \quad k = 1 \dots N \quad (13)$$

In the limit as N goes to infinity, one can deduce that r approaches a constant value r_∞ , and ψ rotates at the mean frequency of $g(w)$. Without loss of generality, we let $\psi = 0$ by entering an appropriate frame rotating at that mean frequency. Thus, we can reduce the dynamics of an individual oscillator to the following autonomous form:

$$\dot{\theta}_k = \omega_k - K r \sin(\theta_k), \quad k = 1 \dots N \quad (14)$$

When $|\omega_k| \leq K r$, equation (14) has a globally attractive equilibrium at $\theta_k = \sin^{-1}(\frac{\omega_k}{K r})$.

Thus, the set of oscillators $\{\theta_k : |\omega_k| \leq Kr\}$ form a “synchronized cluster” which are all fixed in the rotating frame. On the other hand, oscillators with $|\omega_k| > Kr$ have no steady state equilibrium and will drift around the circle, faster while approaching the synchronized cluster and slower when moving away, but always lapping (or being lapped by) the cluster indefinitely.

Note the similarities and differences between Kuramoto’s approach and Wu and Chua’s approach. Both derived conditions for synchronization by finding a lower bound on the coupling strength which guarantees that cells will synchronize. Additionally, they both use techniques for simplifying the (potentially complex) topography of the coupling network into a reduced form. However, they differ greatly in the mathematical tools used in their analyses and in the models they analyze. Kuramoto focuses on limit cycle oscillators with sinusoidal coupling, while Wu and Chua examine general nonlinear systems with linear coupling.

2.4 Contraction Analysis

Contraction analysis [11] [12] is a modern tool that will allow us to analyze synchronization more easily than the previous sections. Contraction analysis takes a slightly different view of stability: Instead of relating system trajectories to a nominal motion, contraction views stability as whether *all pairs* of system trajectories exponentially approach each other. This approach allows us to handle nonidentical systems, an advantage over the Wu and Chua framework.

This section will summarize the key concepts and theorems from contraction theory and discuss how they can be applied to synchronization. In this review, we will present only the relevant results for our application. Readers interested in a general treatment and proofs of these theorems should refer to Lohmiller & Slotine [11] and Pham & Slotine [12].

The results of this section are expressed in terms of the eigenvalues of the symmetric part of matrices. For a square matrix \mathbf{A} , we call $\mathbf{A}_s = \frac{1}{2}(\mathbf{A}^T + \mathbf{A})$ the symmetric part of \mathbf{A} . \mathbf{A} is called *positive definite* (*negative definite*) if each eigenvalue of \mathbf{A}_s is greater (less) than 0. Denote the greatest (least) eigenvalues of \mathbf{A}_s by $\lambda_{\max}(\mathbf{A})$ ($\lambda_{\min}(\mathbf{A})$). $\mathbf{A}(\mathbf{x}, t)$ is *uniformly positive definite* (*uniformly negative definite*) if there exists $\beta > 0$ such that for all \mathbf{x}, t , $\lambda_{\min}(\mathbf{A}(\mathbf{x}, t)) > \beta$ ($\lambda_{\max}(\mathbf{A}(\mathbf{x}, t)) < -\beta$).

Consider a general nonlinear time-varying system in \mathbb{R}^n

$$\dot{\mathbf{x}} = \mathbf{f}(\mathbf{x}, t) \tag{15}$$

Theorem 5 (Contraction [11]). If there exists a square invertible matrix $\Theta(\mathbf{x}, t)$ such that $\mathbf{M} = \Theta(\mathbf{x}, t)^T \Theta(\mathbf{x}, t)$ is uniformly positive definite, and $\mathbf{F} = \left(\dot{\Theta} + \Theta \frac{\partial \mathbf{f}}{\partial \mathbf{x}} \right) \Theta^{-1}$ is uniformly negative definite, then any two trajectories of System (15) exponentially approach each other with rate $\lambda = |\sup_{\mathbf{x}, t} \lambda_{\max}(\mathbf{F})|$. System (15) is called *contracting* with respect to \mathbf{x} , \mathbf{F} is called the *generalized Jacobian*, λ is the *contraction rate*, and \mathbf{M} is the *contraction metric*.

Theorem 6 (Contraction and Robustness [11]). Suppose System (15) is contracting with metric \mathbf{I} and rate λ . Let $\mathbf{x}_1(t)$ be a trajectory of the system, and let $\mathbf{x}_2(t)$ be a trajectory of the perturbed system $\dot{\mathbf{x}} = \mathbf{f}(\mathbf{x}, t) + \mathbf{p}(\mathbf{x}, t)$. Then, after exponential transients of rate λ , the following inequality holds

$$\|\mathbf{x}_1(t) - \mathbf{x}_2(t)\| \leq \sup_{\mathbf{x}, t} \frac{\|\mathbf{p}(\mathbf{x}, t)\|}{\lambda}$$

Now, we can turn our attention to the results of [12].

Theorem 7 (Contraction to a Subspace [12]). For System (15), suppose that there exists a *flow-invariant subspace* \mathcal{M} of dimension p . That is, $\mathbf{f}(\mathbf{x}, t) \in \mathcal{M}$ for all $\mathbf{x} \in \mathcal{M}$ and $t \in \mathbb{R}^+$. Let $\{\mathbf{u}_1, \mathbf{u}_2, \dots, \mathbf{u}_p\}$ be an orthonormal basis of \mathcal{M} , and let $\{\mathbf{v}_1, \mathbf{v}_2, \dots, \mathbf{v}_{n-p}\}$ be an orthonormal basis of the orthogonal subspace \mathcal{M}^\perp . Construct the matrices \mathbf{U} and \mathbf{V} , whose rows are $\mathbf{u}_1^T, \mathbf{u}_2^T, \dots, \mathbf{u}_p^T$ and $\mathbf{v}_1^T, \mathbf{v}_2^T, \dots, \mathbf{v}_{n-p}^T$ respectively. A particular solution $\mathbf{x}_p(t)$ converges to \mathcal{M} if the system

$$\dot{\mathbf{y}} = \mathbf{V} \mathbf{f}(\mathbf{V}^T \mathbf{y} + \mathbf{U}^T \mathbf{U} \mathbf{x}_p(t), t) \quad (16)$$

is contracting with respect to \mathbf{y} . If this condition is fulfilled for all solutions $\mathbf{x}_p(t)$, then all solutions of System (15) exponentially converge to \mathcal{M} . If, furthermore, the contraction rates of (16) are lower-bounded by λ , then the convergence will be exponential with rate λ .

Corollary 7.1. A sufficient condition for exponential convergence to \mathcal{M} is that there exists an invertible transform Θ on \mathcal{M} such that

$$\Theta \mathbf{V} \frac{\partial \mathbf{f}}{\partial \mathbf{x}} \mathbf{V}^T \Theta^{-1} < 0 \quad \forall \mathbf{x}, t \quad (17)$$

Recall the setup in section 2.2, with the coupled identical systems of equation (2) and the compact form of equation (3). The set of synchronized states is defined by the linear equality constraints $\mathbf{x}_i = \mathbf{x}_{i+1}$, $i = 1 \dots m - 1$, which implicitly defines a *synchronized subspace* we will call \mathcal{M} . On the synchronized subspace, the coupling forces disappear, which means that

\mathcal{M} is flow-invariant. This observation directly leads to the following theorem

Theorem 8 (Synchronization via Contraction [12]). Consider coupled systems in the compact form of equation (3). Let \mathbf{V} be a matrix whose rows form an orthonormal basis for the orthogonal complement to the synchronized subspace¹. If there exists a constant invertible square matrix Θ such that

$$\Theta \mathbf{V} \left(\begin{bmatrix} \frac{\partial \mathbf{f}}{\partial \mathbf{x}}(\mathbf{x}_1, t) & \mathbf{0} & \mathbf{0} \\ \mathbf{0} & \ddots & \mathbf{0} \\ \mathbf{0} & \mathbf{0} & \frac{\partial \mathbf{f}}{\partial \mathbf{x}}(\mathbf{x}_m, t) \end{bmatrix} + \mathbf{D} \right) \mathbf{V}^T \Theta^{-1} < 0 \quad \forall \mathbf{x}, t \quad (18)$$

then System (2) globally exponentially synchronizes. The contraction rate of the auxiliary system is the *synchronization rate*.

Proof. Follows from observing that $\frac{\partial \bar{\mathbf{f}}}{\partial \bar{\mathbf{x}}}(\bar{\mathbf{x}}, t) = \text{diag}\left(\frac{\partial \mathbf{f}}{\partial \mathbf{x}}(\mathbf{x}_1, t), \dots, \frac{\partial \mathbf{f}}{\partial \mathbf{x}}(\mathbf{x}_m, t)\right) + \mathbf{D}$, and applying corollary 7.1. \square

Corollary 8.1. More specifically, if

$$\lambda_{\min}(-\mathbf{V} \mathbf{D} \mathbf{V}^T) > \sup_{\mathbf{a}, t} \lambda_{\max}\left(\frac{\partial \mathbf{f}}{\partial \mathbf{x}}(\mathbf{a}, t)\right) \quad (19)$$

then System (2) globally exponentially synchronizes.

Proof. Since \mathbf{V} is orthonormal,

$$\sup_{\mathbf{a}, t} \lambda_{\max}\left(\frac{\partial \mathbf{f}}{\partial \mathbf{x}}(\mathbf{a}, t)\right) \geq \lambda_{\max}\left(\mathbf{V} \begin{bmatrix} \frac{\partial \mathbf{f}}{\partial \mathbf{x}}(\mathbf{x}_1, t) & \mathbf{0} & \mathbf{0} \\ \mathbf{0} & \ddots & \mathbf{0} \\ \mathbf{0} & \mathbf{0} & \frac{\partial \mathbf{f}}{\partial \mathbf{x}}(\mathbf{x}_m, t) \end{bmatrix} \mathbf{V}^T\right)$$

So the inequality (19) implies negative definiteness of equation (18) for $\Theta = \mathbf{I}$. \square

Note that these theorems do not say anything about the stability of individual dynamics. In fact, it is possible that the individual systems have unbounded growth while collectively remaining on the synchronized subspace.

¹The synchronization constraints are a tempting choice for directly forming the bases in \mathbf{U} and \mathbf{V} , but are not generally orthonormal. In practice, one can use a Gram-Schmidt process to obtain the desired orthonormal basis from the synchronization constraints

One more theorem is provided for coupled systems which are non-identical. Consider the following setup

$$\dot{\mathbf{x}}_i = \mathbf{f}_i(\mathbf{x}_i, t) + \sum_{j=1}^m \mathbf{D}_{i,j} \mathbf{x}_j \quad i = 1 \dots m \quad (20)$$

Let $\mathbf{c}(\mathbf{x}, t)$ be the center of the smallest ball that contains each $\mathbf{f}_i(\mathbf{x}, t)$. Further, define $\mathbf{p}_i(\mathbf{x}, t)$ such that $\mathbf{f}_i(\mathbf{x}, t) = \mathbf{c}(\mathbf{x}, t) + \mathbf{p}_i(\mathbf{x}, t)$ for $i = 1 \dots m$. We write the compact dynamics as

$$\dot{\bar{\mathbf{x}}} = \bar{\mathbf{c}}(\bar{\mathbf{x}}, t) + \mathbf{D}\bar{\mathbf{x}} + \bar{\mathbf{p}}(\bar{\mathbf{x}}, t) \quad (21)$$

Theorem 9 (Robust Synchronization [12]). Suppose that the system $\dot{\bar{\mathbf{x}}} = \bar{\mathbf{c}}(\bar{\mathbf{x}}) + \mathbf{D}\bar{\mathbf{x}}$ exponentially synchronizes with rate λ . Then after exponential transients, any trajectory of system (21) will be contained within a distance of $\sup_{\bar{\mathbf{x}}, t} \frac{\|\mathbf{V}\bar{\mathbf{p}}(\bar{\mathbf{x}}, t)\|}{\lambda}$ from the subspace \mathcal{M} .

2.5 Noisy Coupled Systems

The 2010 paper by Tabareau, Slotine, and Pham titled *How Synchronization Protects from Noise* [4] attempts to formalize the notion of *collective enhancement of precision* [13] in coupled systems. They use a stochastic differential equations approach, which is beyond the scope of this thesis. However, this section will briefly present the setup and results of their paper, and section 3.4 will present simulation results which illuminate these ideas.

Consider the network of coupled noisy cells

$$d\mathbf{x}_i = \left(\mathbf{f}(\mathbf{x}_i, t) + \sum_{j \neq i} \mathbf{K}_{ji}(\mathbf{x}_j - \mathbf{x}_i) \right) dt + \sigma dW_i, \quad i = 1 \dots m \quad (22)$$

Consider the following assumptions about system (22)

B1 The network is balanced, i.e. $\forall i \quad \sum_j \mathbf{K}_{ji} = \sum_j \mathbf{K}_{ij}$.

B2 The nonlinearity of \mathbf{f} is bounded. Specifically, If the Hessian of $\mathbf{f}^{(j)}$ is \mathbf{H}_j , then there exists a constant scalar H_b such that $\lambda_{\max}(\mathbf{H}_j) \leq \frac{1}{\sqrt{m}} H_b$ for all \mathbf{x}, j . Note that for a linear system, $\mathbf{H}_j = \mathbf{0}$ uniformly, so $H_b = 0$.

B3 The noise-free system $\dot{\mathbf{x}}_{nf} = \mathbf{f}(\mathbf{x}_{nf}, t)$ is contracting (see section 2.4).

B4 The expected squared distance between states is bounded. Specifically, after exponential transients, there exists ρ such that $\mathbb{E} \left(\sum_{i=1}^{m-1} \|\mathbf{x}_i - \mathbf{x}_{i+1}\|^2 \right) \leq \rho$

Theorem 10 (Effect of Noise [4]). If assumptions **B1** - **B4** hold for system (22), then when $m \rightarrow \infty$ and $\frac{\rho}{m^2} \rightarrow 0$, the distance between any noisy cell $\mathbf{x}_i(t)$ and the noise free system $\mathbf{x}_{nf}(t)$ tends to 0. Furthermore, the impact of noise on the distance between the the noise free trajectory $\mathbf{x}_{nf}(t)$ and the mean trajectory $\frac{1}{m} \sum_{i=1}^m \mathbf{x}_i(t)$ evolves as

$$\frac{\rho H_b}{2m^2} + \frac{\sigma}{\sqrt{m}} \quad (23)$$

The key observation here is that ρ and H_b appear together in equation (23). This means that when $\mathbf{f}(\mathbf{x}, t) = \mathbf{A}\mathbf{x} + \mathbf{u}(t)$, the first term equals 0, and the impact of noise *only* depends on the noise intensity σ and the number of cells m . Interestingly, this implies that for linear cells, coupling should offer no protection from noise. Rather, cells are protected from noise by virtue of being linear. Additionally, they gain protection by increasing the number of cells m .

In the large m limit, it is tempting to assume that the right term dominates the left in equation (23) since $\frac{1}{m^2} \ll \frac{1}{\sqrt{m}}$ as $m \rightarrow \infty$. However, this would neglect the fact that the synchronization bound ρ could grow with m . If ρ is $\mathcal{O}(m^{1.5})$ (using big-O notation), then the left term would not be dominated in the large m limit.

2.6 Diffusion

Diffusion is an ubiquitous process in biological systems, and will form the basis of our modeling of neuron interactions. Fick's first law of diffusion for an ideal dilute solution states that the diffusive flux j is related to the concentration at a point $c(x, y, z)$ and the diffusivity δ (which is a function of temperature, viscosity, chemical properties, etc.), with ∇ denoting the gradient operator as follows [14]:

$$j = -\delta \nabla c(x, y, z) \quad (24)$$

This can be simply understood to mean that chemicals move from high-concentration area's to low concentration areas. If there are multiple solute's present, at low concentrations we

can model the diffusion of each as independent of the rest [14]. We can rewrite Fick's law for a vector of concentrations $\mathbf{c} = [c^{(1)}, c^{(2)}, \dots, c^{(n)}]^T$ and corresponding vector of fluxes \mathbf{j} as

$$\mathbf{j} = - \begin{bmatrix} \delta^{(1)} & & & \\ & \delta^{(2)} & & \\ & & \ddots & \\ & & & \delta^{(n)} \end{bmatrix} \nabla \mathbf{c}(x, y, z) \quad (25)$$

Consider two well-mixed cells of equal volume separated by a permeable membrane of negligible thickness. Assume that the concentration is uniform within each cell and let \mathbf{c}_1 and \mathbf{c}_2 denote the concentration vectors of the first and second cells respectively. Fick's first law can be rewritten as the following linear ordinary differential equation

$$\dot{\mathbf{c}}_1 = \mathbf{D}(\mathbf{c}_2 - \mathbf{c}_1) \quad (26)$$

$$\dot{\mathbf{c}}_2 = \mathbf{D}(\mathbf{c}_1 - \mathbf{c}_2) \quad (27)$$

Where \mathbf{D} is a diagonal membrane diffusivity matrix given by $\text{diag}(d_1, d_2, \dots, d_n)$, which is now a function of membrane properties and geometry, as well as temperature, viscosity, chemical properties, etc [14].

3 Results

3.1 Modeling Neuron Interactions

We model the parallel filters from Figure 1 as m cells whose states \mathbf{x}_i are a vector of concentrations of n chemical species. Each cell receives the same input \mathbf{u} , and implements the filter $\dot{\mathbf{x}}_i = \mathbf{f}_i(\mathbf{x}_i, t) = \mathbf{F}_i \mathbf{x}_i + \mathbf{G} \mathbf{u}$. The cells are arranged in a ring, and connected to their k nearest neighbors on both sides as shown in Figure 2. Each edge represents a shared permeable membrane. We assume that the exchange of concentration at each membrane can be modeled by equations (26) - (27), and that the membrane diffusivity matrix is the same at each edge. Let $N(\mathbf{x}_j)$ denote the set of cells sharing an edge with cell \mathbf{x}_j , then we can write the model as follows:

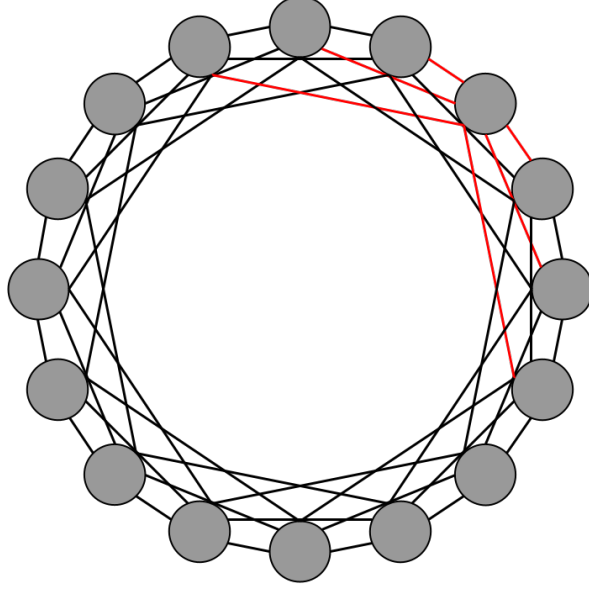


Figure 2: Example k -connected ring with $m = 16$ and $k = 3$. Edges for one vertex are highlighted red to show that each node is connected to the k -nearest neighbors on both sides.

$$\begin{aligned}
 \dot{\mathbf{x}}_1 &= \mathbf{f}_1(\mathbf{x}_1) + \sum_{\mathbf{x}_i \in N(\mathbf{x}_1)} \mathbf{D}(\mathbf{x}_i - \mathbf{x}_1) \in \mathbb{R}^n \\
 &\vdots \\
 \dot{\mathbf{x}}_m &= \mathbf{f}_m(\mathbf{x}_m) + \sum_{\mathbf{x}_i \in N(\mathbf{x}_m)} \mathbf{D}(\mathbf{x}_i - \mathbf{x}_m) \in \mathbb{R}^n
 \end{aligned} \tag{28}$$

This can be easily adapted to the form of Wu and Chua's framework by letting $\text{circ}(\mathbf{r})$ define the circulant matrix whose first row is \mathbf{r} , and writing

$$\mathbf{x} := \begin{bmatrix} \mathbf{x}_1 \\ \vdots \\ \mathbf{x}_m \end{bmatrix} \quad \bar{\mathbf{f}}(\mathbf{x}) := \begin{bmatrix} \mathbf{f}(\mathbf{x}_1) \\ \vdots \\ \mathbf{f}(\mathbf{x}_m) \end{bmatrix} \quad \bar{\mathbf{D}} := \text{circ} \left(\begin{bmatrix} -k\mathbf{D} & \mathbf{D} & \dots & \mathbf{D} & \mathbf{0} & \dots & \mathbf{0} & \mathbf{D} & \dots & \mathbf{D} \end{bmatrix} \right)$$

we can rewrite (2) as

$$\dot{\mathbf{x}} = \bar{\mathbf{f}}(\mathbf{x}) + \bar{\mathbf{D}}\mathbf{x} \in \mathbb{R}^{nm} \tag{29}$$

3.2 Synchronization in Neuron Model

Using the results from section 2.2.5, it is straightforward to derive synchronization conditions for this model. Observe that each \mathbf{D} is diagonal, and properties **A1-A5** are satisfied for each $\tilde{\mathbf{D}}$. Since $\tilde{\mathbf{D}}$ is circulant, its eigenvalues λ_j are given by the discrete Fourier transform of the first row [5]. We can easily compute them as:

$$\lambda_j = d_i \left(-2k + \sum_{l=1}^k \exp\left(\frac{2\pi l j i}{m}\right) + \sum_{l=m-k}^{m-1} \exp\left(\frac{2\pi l j i}{m}\right) \right) \quad (30)$$

The greatest non-zero real part $Re(\lambda_{\max})$ is given by:

$$Re(\lambda_{\max}) = d_i \left(-2k + \sum_{l=1}^k \cos\left(\frac{2\pi l i}{m}\right) + \sum_{l=m-k}^{m-1} \cos\left(\frac{2\pi l i}{m}\right) \right) \quad (31)$$

Therefore, by Theorem 4, the cells will asymptotically synchronize if:

$$d_i \left(2k - \sum_{l=1}^k \cos\left(\frac{2\pi l}{m}\right) - \sum_{l=m-k}^{m-1} \cos\left(\frac{2\pi l}{m}\right) \right) \geq t_i \quad (32)$$

Recall that t_i will be related to the amount of negative state feedback required to stabilize a single cell, which is determined by the Jacobian of $\mathbf{f}_i(\mathbf{x}_i)$. The other side of the equation is purely dependent upon the diffusivity of the membrane to a particular chemical species d_i and the coupling parameters m and k .

3.3 Main result for linear systems

In this section, we apply the ideas developed in section 2 to the problem of coupled non-identical linear systems. The main result is a theorem providing necessary and sufficient conditions for approximate synchronization and stability of such systems. The proof uses ideas from [12], as well as classical results from linear systems theory [15].

Consider an array of m linearly coupled non-identical cells, as in system (20). However, we will assume that these cells are linear and receive a shared vector-valued input $\mathbf{u}(t)$. That is, $\mathbf{f}_i(\mathbf{x}_i, t) = \mathbf{A}_i \mathbf{x}_i + \mathbf{u}(t)$. Define $\mathbf{C} = \frac{1}{m} \sum_{i=1}^m \mathbf{A}_i$, and $\mathbf{P}_i = \mathbf{A}_i - \mathbf{C}$. Further, let $\bar{\mathbf{P}} = \text{diag}(\mathbf{P}_1, \dots, \mathbf{P}_m)$ and let $\bar{\mathbf{C}} = \text{diag}(\mathbf{C}, \dots, \mathbf{C})$. Finally, let $\mathbf{B} = \begin{bmatrix} \mathbf{I} & \mathbf{I} & \dots & \mathbf{I} \end{bmatrix}^T$.

Then we can rewrite system (20) as

$$\dot{\bar{\mathbf{x}}} = (\bar{\mathbf{C}} + \bar{\mathbf{P}} + \mathbf{D})\bar{\mathbf{x}} + \mathbf{B}\mathbf{u}(t) \quad (33)$$

As in section 2.4, let \mathcal{M} represent the synchronized subspace, and let \mathbf{U} and \mathbf{V} be matrices whose rows form orthonormal bases for \mathcal{M} and \mathcal{M}^\perp , respectively.

Theorem 11. The system represented in equation (33) will, after exponential transients, be contained within a finite boundary of the synchronization subspace **and** be asymptotically stable if and only if the eigenvalues of the matrices $\bar{\mathbf{C}} + \bar{\mathbf{P}} + \mathbf{D}$ and $\mathbf{V}(\bar{\mathbf{C}} + \bar{\mathbf{P}} + \mathbf{D})\mathbf{V}^T$ all have negative real parts and the input $\mathbf{u}(t)$ is bounded.

Proof. Define $\mathbf{z} = \mathbf{V}\bar{\mathbf{x}}$. Note that $\bar{\mathbf{x}}$ is on the synchronized subspace if and only if $\mathbf{z} = \mathbf{0}$. The dynamics of \mathbf{z} are $\dot{\mathbf{z}} = \mathbf{V}(\bar{\mathbf{C}} + \bar{\mathbf{P}} + \mathbf{D})\bar{\mathbf{x}} + \mathbf{V}\mathbf{B}\mathbf{u}(t)$. Note that the columns of \mathbf{B} are on the synchronized subspace, so $\mathbf{V}\mathbf{B} = \mathbf{0}$. Additionally, since \mathbf{V} and \mathbf{U} together form an orthonormal basis of \mathbb{R}^n , $\mathbf{V}^T\mathbf{V} + \mathbf{U}^T\mathbf{U} = \mathbf{I}$. So we can rewrite the dynamics of \mathbf{z} as

$$\dot{\mathbf{z}} = \mathbf{V}(\bar{\mathbf{C}} + \bar{\mathbf{P}} + \mathbf{D})\mathbf{V}^T\mathbf{z} + \mathbf{V}(\bar{\mathbf{C}} + \bar{\mathbf{P}} + \mathbf{D})\mathbf{U}^T\mathbf{U}\bar{\mathbf{x}} \quad (34)$$

Since $\mathbf{U}^T\mathbf{U}$ is a projection onto the synchronized subspace, we know that $\mathbf{D}\mathbf{U}^T\mathbf{U}\bar{\mathbf{x}} = \mathbf{0}$. Additionally, $\bar{\mathbf{C}}\mathbf{U}^T\mathbf{U}\bar{\mathbf{x}}$ is on the synchronized subspace, so $\mathbf{V}\bar{\mathbf{C}}\mathbf{U}^T\mathbf{U}\bar{\mathbf{x}} = \mathbf{0}$, allowing us to simplify equation (34).

Now we can write the overall dynamics for $\bar{\mathbf{x}}$ and \mathbf{z}

$$\begin{bmatrix} \dot{\bar{\mathbf{x}}} \\ \dot{\mathbf{z}} \end{bmatrix} = \begin{bmatrix} \bar{\mathbf{C}} + \bar{\mathbf{P}} + \mathbf{D} & \mathbf{0} \\ \mathbf{V}\bar{\mathbf{P}}\mathbf{U}^T\mathbf{U} & \mathbf{V}(\bar{\mathbf{C}} + \bar{\mathbf{P}} + \mathbf{D})\mathbf{V}^T \end{bmatrix} \begin{bmatrix} \bar{\mathbf{x}} \\ \mathbf{z} \end{bmatrix} + \begin{bmatrix} \bar{\mathbf{B}} \\ \mathbf{0} \end{bmatrix} \mathbf{u}(t) \quad (35)$$

This system is asymptotically stable if and only if the eigenvalues of the diagonal blocks $\bar{\mathbf{C}} + \bar{\mathbf{P}} + \mathbf{D}$ and $\mathbf{V}(\bar{\mathbf{C}} + \bar{\mathbf{P}} + \mathbf{D})\mathbf{V}^T$ all have negative real parts [15]. Additionally, the state \mathbf{z} is bounded if the input $\mathbf{u}(t)$ is bounded, which implies that the distance between \mathbf{x} and the synchronized subspace is bounded. \square

Note that these results are for coupled non-identical noise-free linear systems, while section 2.5 explores coupled identical noisy linear systems. No results covered in this paper thus

far pertain to the effect of noise on coupled, non-identical, noisy, linear systems. The next section attempts to address this gap using simulations, and contains a surprising finding.

3.4 Simulations

3.4.1 Methods

Simulations were conducted investigating the role of linearity, perturbation, noise, coupling, and the number of cells in a network. Results were obtained using MATLAB and Simulink: a link to the codebase used is provided in appendix B. In all simulations, the cells are coupled in a bi-directional ring with diffusive coupling $\mathbf{K}_{ij} = k\mathbf{I}_2$. The error energy is computed as the squared distance between the trajectory of an unperturbed, noise-free system and the mean trajectory of coupled noisy cells.

Figures 3(a), 4(a), and 5(a) compare results for identical linear cells of the form $\mathbf{f}(\mathbf{x}_i, t) = \mathbf{C}\mathbf{x}_i + \mathbf{u}(t)$ with non-identical linear cells of the form $\mathbf{f}(\mathbf{x}_i, t) = \mathbf{C}\mathbf{x}_i + \mathbf{P}_i\mathbf{x}_i + \mathbf{u}(t)$.

Figures 3(b), 4(b), and 5(b) compare results for identical nonlinear cells of the form $\mathbf{f}(\mathbf{x}_i, t) = -3 \tanh(\mathbf{x}_i) + \mathbf{u}(t)$ with non-identical nonlinear cells of the form $\mathbf{f}(\mathbf{x}_i, t) = -3 \tanh(\mathbf{x}_i) + \mathbf{P}_i\mathbf{x}_i + \mathbf{u}(t)$.

We use the values $\mathbf{C} = \begin{bmatrix} -3 & 2 \\ 0 & -3.2 \end{bmatrix}$ and $\mathbf{u}(t) = \begin{bmatrix} \sin(t) \\ \sin(t) \end{bmatrix}$. \mathbf{P}_i is a 2×2 matrix whose values are sampled from a scaled gaussian distribution $0.1\mathcal{N}(0, 1)$ [16], making each system non-identical. The error is averaged over 50 trials (re-sampling \mathbf{P}_i each trial).

Figure 3 varies the value of the coupling parameter k from 0 to 15, Figure 4 varies the noise intensity σ from 0 to 3, and Figure 5 varies the number of systems m from 3 to 15. The default values for parameters when they are not the independent variable is $k = 1$, $\sigma = 0.1$, and $m = 15$.

3.4.2 Simulation Results and Discussion

In order to investigate whether theorem 10 (from [4]) applies to non-identical cells, a series of simulations were conducted using MATLAB and Simulink. Figures 3, 4, and 5 compare the impact of noise on coupled *identical* cells with the impact of noise on coupled non-identical cells.

As shown in Figure 3(a), increasing coupling strength (as a proxy for synchronization) does not confer protection from noise on identical linear cells. When the cells are non-identical,

increasing coupling strength *does* protect from noise. This regime (noisy, non-identical cells) is not covered analytically in this paper, so this experimental result is novel. Intuitively, this does make sense, as we expect synchronization to protect cells generally, but it conflicts with our understanding of the effect of synchronization on coupled identical linear cells. Additionally, the correlation is quite small and unclear, despite averaging over 50 trials. This suggests that further investigation is warranted to better understand this regime.

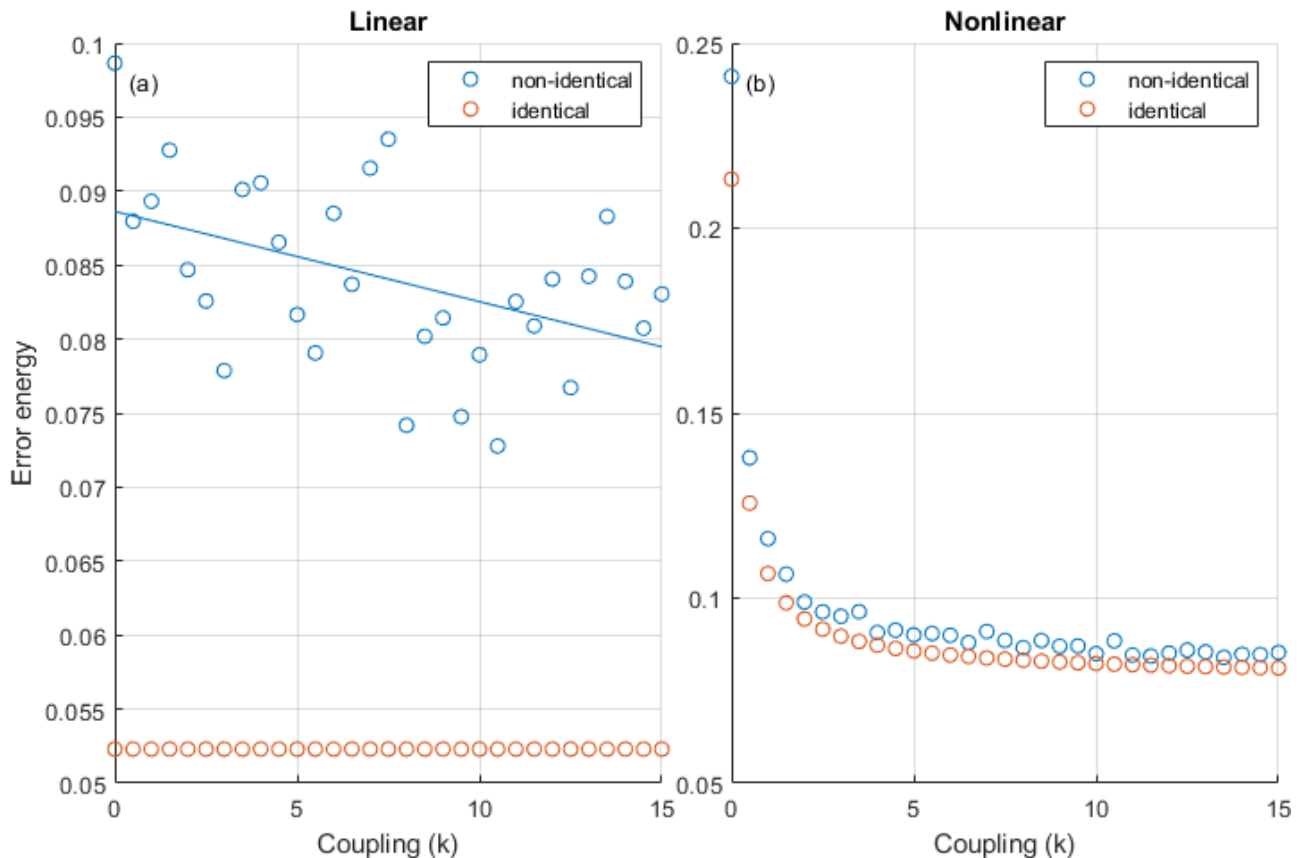


Figure 3: Simulation results for the error between a noise free cell and coupled noisy cells against k , the coupling strength. In (a), the cells dynamics are linear, while in (b) they are nonlinear.

Figure 4 closely follows the predictions of theorem 10, with a few interesting patterns. In the linear-cell case, the relationship between noise intensity and error is strictly linear, while in the nonlinear case the relationship is less exact. This may be due to the impact of noise on the synchronization bound, which introduces additional error through the first term in equation (23).

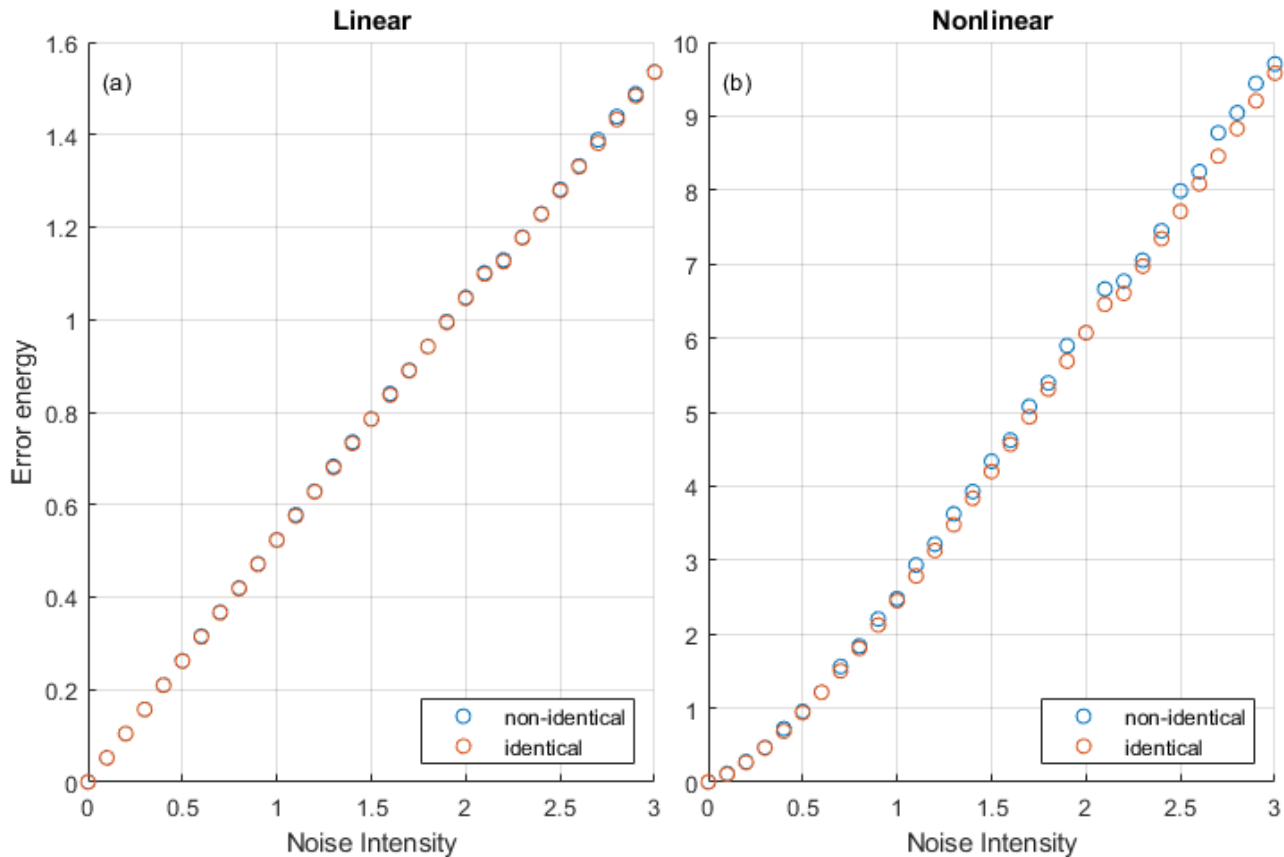


Figure 4: Simulation results for the error between a noise free cell and coupled noisy cells against σ , the noise intensity. In (a), the cells dynamics are linear, while in (b) they are nonlinear.

Finally, the relationship in Figure 5 is somewhat surprising. Generally, the plot appears to follow the $\frac{1}{m^2}$ form that we expect, but there are surprising “bumps” at $m = 9$ which have no clear explanation. This pattern is consistent across linear, nonlinear, identical, and non-identical regimes. While possibly nothing more than a numerical artifact from the simulations, this pattern could warrant further investigation.

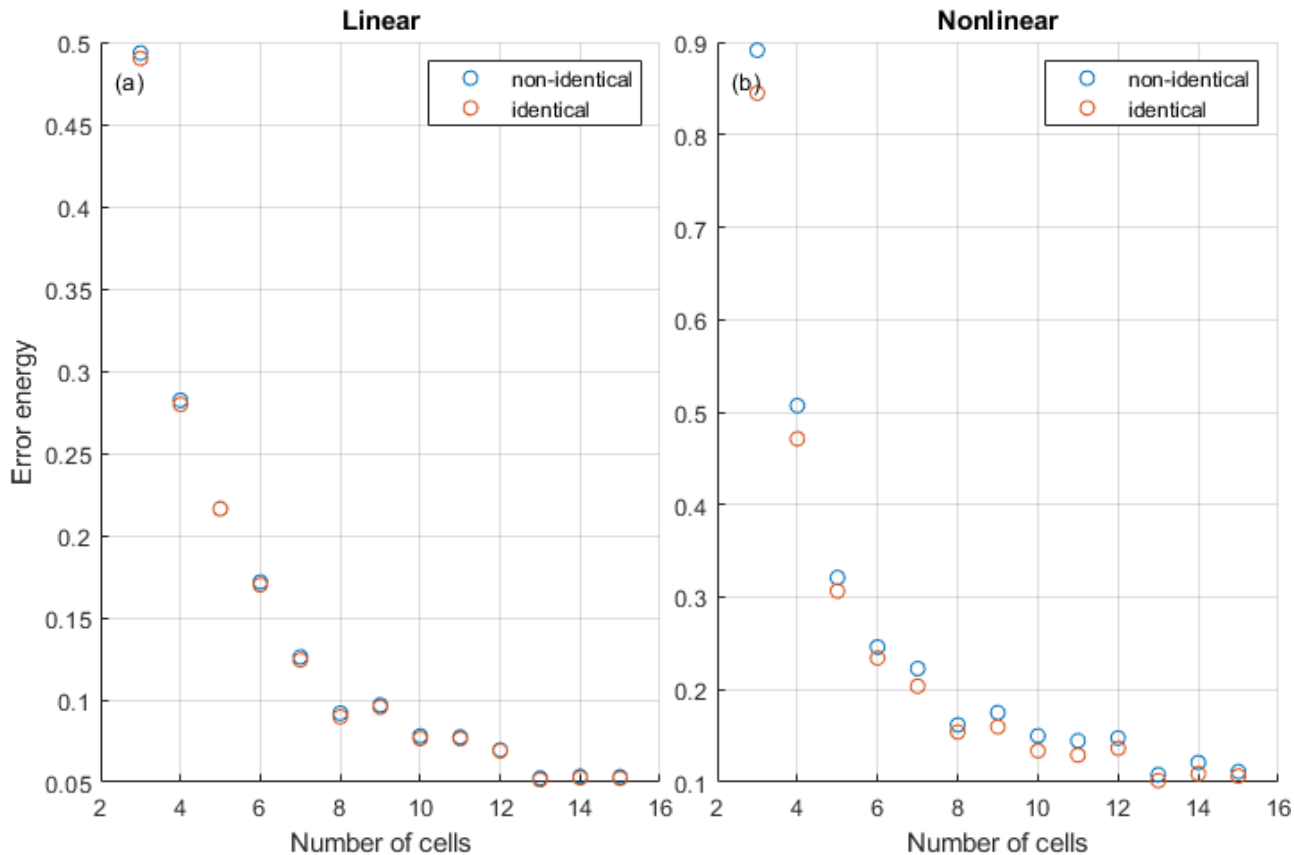


Figure 5: Simulation results for the error between a noise free cell and coupled noisy cells against m . In (a), the cells dynamics are linear, while in (b) they are nonlinear.

4 Further Work

So far we have only attempted to answer Question 2 regarding the impact of noise and perturbation on coupled linear systems. The issue of synchronizing system matrices posed in Question 1 remains open, and it is unclear whether the analysis presented here will be useful in answering it. One potential approach would be to examine that synchronization problem as a multi timescale process, assuming that the synchronization happens much faster than the systems dynamics. This approach could require the use of averaging analysis.

Another gap in this research is that the model presented here for neuron interactions remains speculative, and was not informed by thorough research of existing neuron models. More work will need to be done to verify that the model presented in this paper is accurate. Additionally, it would be valuable to evaluate some of the synchronization conditions presented using numerical estimates of the model parameters. This would need to be done in tandem with further refinements to the model, including more detailed research into the coupling

structure.

Finally, further research should be done to understand the results of the simulations on coupled, non-identical, noisy systems. While this thesis has covered results concerning coupled identical noisy systems and coupled non-identical noise-free systems, combining these results was only analyzed in simulations which produced interesting results. These results should be investigated using more detailed simulations and background research.

5 Conclusion

This thesis looked at a model of the human cerebellum, and identified problems related to the role of synchronization in that model. We looked at several frameworks for analyzing synchronization in coupled systems, comparing and contrasting them. Then, we developed models of the coupled neurons, and analyzed them through the mentioned framework. This allowed us to derive analytic synchronization conditions. Additionally, simulations were conducted to validate theoretical results on the role of noise and perturbation in coupled systems, as well as investigate problems for which no theoretical results were available.

References

- [1] M. W. Spong, S. Hutchinson, and M. Vidyasagar, *Robot Modelling and control*. John Wiley & Sons, 2005.
- [2] M. E. Broucke, “Adaptive internal models in neuroscience,” *Foundations and Trends® in Systems and Control*, vol. 9, no. 4, pp. 365–550, 2022. [Online]. Available: <http://dx.doi.org/10.1561/26000000027>
- [3] S. J. Schiff, *Neural control engineering: The emerging intersection between Control Theory and neuroscience*. MIT Press, 2022.
- [4] N. Tabareau, J.-J. Slotine, and Q.-C. Pham, “How synchronization protects from noise,” *PLOS Computational Biology*, vol. 6, no. 1, pp. 1–9, 01 2010. [Online]. Available: <https://doi.org/10.1371/journal.pcbi.1000637>
- [5] C. W. Wu and L. Chua, “Synchronization in an array of linearly coupled dynamical systems,” *IEEE Transactions on Circuits and Systems I: Fundamental Theory and Applications*, vol. 42, no. 8, pp. 430–447, 1995.
- [6] C. Wu and L. O. Chua, “A unified framework for synchronization and control of dynamical systems,” UC Berkeley, EECS, Tech. Rep. UCB/ERL M94/28, Jan 1994. [Online]. Available: <http://www2.eecs.berkeley.edu/Pubs/TechRpts/1994/2540.html>
- [7] F. R. K. Chung, *Spectral Graph Theory*. American Mathematical Society, 1997.
- [8] J. Slotine and W. Li, *Fundamentals of Lyapunov Theory*. Prentice-Hall International, 1991, p. 40–97.
- [9] S. Boyd and L. Vandenberghe, *Introduction to applied linear algebra: Vectors, matrices, and least squares*. Cambridge University Press, 2023.
- [10] S. H. Strogatz, “From kuramoto to crawford: exploring the onset of synchronization in populations of coupled oscillators,” *Physica D: Nonlinear Phenomena*, vol. 143, no. 1, pp. 1–20, 2000. [Online]. Available: <https://www.sciencedirect.com/science/article/pii/S0167278900000944>
- [11] W. LOHMILLER and J.-J. E. SLOTINE, “On contraction analysis for non-linear systems,” *Automatica*, vol. 34, no. 6, pp. 683–696, 1998. [Online]. Available: <https://www.sciencedirect.com/science/article/pii/S0005109898000193>

- [12] Q. C. Pham and J.-J. Slotine, “Stable concurrent synchronization in dynamic system networks,” *Neural networks : the official journal of the International Neural Network Society*, vol. 20, pp. 62–77, 02 2007.
- [13] D. Needleman, P. Tiesinga, and T. Sejnowski, “Collective enhancement of precision in networks of coupled oscillators,” *Physica D: Nonlinear Phenomena*, vol. 155, pp. 324–336, 07 2001.
- [14] G. Truskey, F. Yuan, and D. Katz, *Transport Phenomena in Biological Systems*, ser. Pearson Prentice Hall bioengineering. Pearson Prentice Hall, 2009. [Online]. Available: <https://books.google.com/books?id=ufMoVsqdTxEC>
- [15] M. H. P. a. Harry L. Trentelman PhD, Anton A. Stoorvogel PhD, *Control Theory for Linear Systems*, 1st ed., ser. Communications and Control Engineering. Springer, 2001.
- [16] “Matlab help center: randn, normally distributed random numbers.” [Online]. Available: <https://www.mathworks.com/help/matlab/ref/randn.html>

A Additional Results from Wu and Chua

A.1 Reducible Coupling Matrix

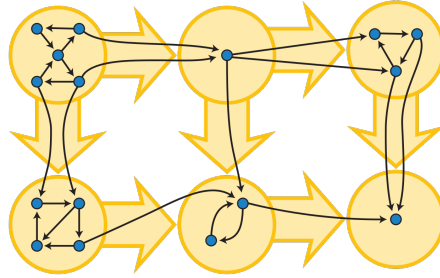


Figure 6: Example of a graph partitioned into strongly connected components, which form the vertices of a directed acyclic graph (Credit Wikimedia)

Suppose the coupling matrix \mathbf{D} is reducible. That is, it can be permuted to a block triangular matrix with irreducible diagonal blocks. If we interpret \mathbf{D} as a directed graph, that means that the graph can be partitioned into strongly connected components, which form the vertices of a directed acyclic graph. Figure 6 show's an example of such a partitioning. In this case, we can study each irreducible partition independently. If we find that the irreducible partitions asymptotically synchronize when uncoupled, then we can “collapse” each one into single cells, and study the behavior of the resulting acyclic directed graph. Consider the example of three strongly connected components (which can easily be extended to an arbitrary number of strongly connected components):

$$\mathbf{c}_1 = \begin{bmatrix} \mathbf{x}_1 \\ \vdots \\ \mathbf{x}_a \end{bmatrix}, \quad \mathbf{c}_2 = \begin{bmatrix} \mathbf{x}_{a+1} \\ \vdots \\ \mathbf{x}_b \end{bmatrix}, \quad \mathbf{c}_3 = \begin{bmatrix} \mathbf{x}_{b+1} \\ \vdots \\ \mathbf{x}_m \end{bmatrix} \quad (36)$$

This result says that if an irreducible subsystem asymptotically synchronizes, then we can treat the irreducible subsystem as a single cell. This fact relates back to an earlier claim that at the synchronized state the dynamics of each cell are the same as the dynamics of an uncoupled cell.

A.2 Nonlinear Additive Coupling

Finally, the paper concludes with some brief results for the more general case of nonlinear additive coupling of the following form

$$\begin{aligned} \dot{\mathbf{x}}_1 &= \mathbf{f}(\mathbf{x}_1) + \mathbf{g}_1(\mathbf{x}) \\ &\vdots \\ \dot{\mathbf{x}}_m &= \mathbf{f}(\mathbf{x}_m) + \mathbf{g}_m(\mathbf{x}) \end{aligned} \tag{45}$$

We can derive similar results as before by assuming a couple facts

1. If $d(\mathbf{x}) = 0$, then $\mathbf{g}_1(\mathbf{x}) = \dots = \mathbf{g}_m(\mathbf{x}) = \mathbf{0} \in \mathbb{R}^n$
2. Each \mathbf{g}_i is differentiable

By a similar proof to the one sketched out in section 2.2.2, we can show that the system will asymptotically synchronize if

$$\mathbf{x}^T \mathbf{U} \left(\begin{array}{c} \left[\begin{array}{c} \mathbf{g}_1(\mathbf{x}) \\ \mathbf{g}_2(\mathbf{x}) \\ \vdots \\ \mathbf{g}_m(\mathbf{x}) \end{array} \right] + \left[\begin{array}{cccc} \mathbf{T} & & & \\ & \mathbf{T} & & \\ & & \ddots & \\ & & & \mathbf{T} \end{array} \right] \mathbf{x} \end{array} \right) \tag{46}$$

is negative semi definite. Furthermore, if we write

$$\mathbf{D}_{i,j}(\mathbf{x}) = \frac{\partial \mathbf{g}_i}{\partial \mathbf{x}_j} \quad (47)$$

$$\mathbf{D}(\mathbf{x}) = \begin{bmatrix} \mathbf{D}_{1,1}(\mathbf{x}) & \dots & \mathbf{D}_{1,m}(\mathbf{x}) \\ \vdots & \ddots & \vdots \\ \mathbf{D}_{m,1}(\mathbf{x}) & \dots & \mathbf{D}_{m,m}(\mathbf{x}) \end{bmatrix} \quad (48)$$

then we can instead check if the matrix

$$\mathbf{U} \left(\mathbf{D}(\mathbf{x}) + \begin{bmatrix} \mathbf{T} & & & \\ & \mathbf{T} & & \\ & & \ddots & \\ & & & \mathbf{T} \end{bmatrix} \right) \quad (49)$$

is negative semidefinite for all \mathbf{x} .

B Simulation Code

https://drive.google.com/drive/folders/1H7fU6dAyY1_K9GVxd8SY99L2j6X5URAj?usp=sharing